

Description of isospin mixing by a generator coordinate method

M. Kimura*

Department of Physics, Hokkaido University, Sapporo 060-0810, Japan
Nuclear Reaction Data Centre, Hokkaido University, Sapporo 060-0810, Japan and
Research Center for Nuclear Physics (RCNP),
Osaka University, Ibaraki 567-0047, Japan

Y. Suzuki

Department of Physics, Hokkaido University, 060-0810 Sapporo, Japan

T. Baba

Kitami Institute of Technology, 090-8507 Kitami, Japan

Y. Taniguchi

Department of Information Engineering,
National Institute of Technology (KOSEN),
Kagawa College, 769-1192 Mitoyo, Japan and
Research Center for Nuclear Physics (RCNP),
Osaka University, Ibaraki 567-0047, Japan

(Dated: August 18, 2021)

Abstract

Background: The isospin mixing is an interesting feature of atomic nuclei. It plays a crucial role in the astrophysical nuclear reactions. However, it is not straightforward for variational nuclear structure models to describe it.

Purpose: We propose a tractable method to describe the isospin mixing within a framework of generator coordinate method, and demonstrate its usability.

Method: We generate the basis wave functions by applying the Fermi transition operator to the wave functions of isobars. The superposition of these basis wave functions and variationally obtained wave functions quantitatively describes the isospin mixing.

Results: Using ^{14}N as an example, we demonstrate that our method reasonably describes both $T = 0$ and 1 states and their mixing. Energy spectrum and $E1$ transition strengths are compared with the experimental data to confirm isospin mixing.

Conclusion: The proposed method is effective enough to describe isospin mixing and is useful, for example, when we discuss α capture reactions of $N = Z$ nuclei.

* masaaki@nucl.sci.hokudai.ac.jp

I. INTRODUCTION

The isospin symmetry is a fundamental symmetry of strong interaction and nuclear force. Because of this symmetry, isobars share a group of states having the same value of the total isospin, which are called isobaric analog states [1, 2]. For example, an $N = Z$ nucleus ^{14}N has the $T = 1$ states such as the 0_1^+ state at 2.31 MeV and the 1_2^- state at 8.06 MeV which are the isobaric analog states corresponding to the ground and first excited states of ^{14}C and ^{14}O .

In reality, isospin is an approximate symmetry of atomic nuclei due to the symmetry breaking terms of nuclear force and Coulomb interaction. Consequently, the mixing of the states with different isospin (isospin mixing) occurs especially in the excited states. Above mentioned 1_2^- state of ^{14}N is a well known example of the isospin mixing for which the admixture of the $T = 0$ and 1 states are experimentally confirmed [3, 4].

An interesting side effect of isospin mixing is that on the selection rule of the $E1$ transitions [1]. If there is no isospin mixing, the $E1$ transitions between two $T = 0$ states are forbidden because $E1$ transition operator is purely isovector at the first order of the long wave-length approximation. However, with isospin mixing, the transition occurs due to the small contamination of the $T = 1$ components. It is notable that this allowed $E1$ transition sometimes plays a crucial role in astrophysical reactions [5, 6]. The radiative α capture reactions of $N = Z$ nuclei such as $^{12}\text{C}(\alpha, \gamma)^{16}\text{O}$ reaction [7] are famous examples for this. reactions. The isospin mixing increases the reaction rate, and can affect the evolution of stars and the abundance of the elements.

Thus, the isospin mixing in $N = Z$ nuclei is an interesting issue relevant to astronomical nuclear reactions. However, the description of the isobaric analog states and isospin mixing are not straight forward for the variational models such as Hartree-Fock models. Since the $T = 0$ states are usually more deeply bound than the $T = 1$ states, the energy variation yields only the $T = 0$ states and the $T = 1$ states are hardly obtained. To overcome this problem, several methods and prescriptions have been suggested [8–11]. For example, the isospin projection before the variation [12, 13] is a solid approach to this problem but computationally demanding. Therefore, the development of a simpler but accurate method is desirable.

In this paper, we propose a tractable method to describe isobaric analog states and isospin

mixing within a framework of generator coordinate method. We generate the basis wave functions by applying the Fermi transition operator to the wave functions of isobars. Using ^{14}N as an example, it will be shown that the superposition of thus-obtained wave functions and variationally obtained wave functions quantitatively describes both $T = 0$ and 1 states and the isospin mixing.

This paper is organized as follows. In the next section, we introduce a method to describe isobaric analog states and isospin mixing. In the section III, we present the numerical results for the $T = 0$ and 1 states and their mixing in ^{14}N . Final section summarizes this work.

II. THEORETICAL FRAMEWORK

A. Hamiltonian and variational wave function

We use the A -body Hamiltonian given as,

$$H = - \sum_i^A \frac{\hbar^2 \nabla_i^2}{2m_N} - t_{\text{cm}} + \sum_{i < j}^A v_{NN}(ij) + \sum_{i < j}^Z v_C(ij), \quad (1)$$

where the Gogny D1S density functional [14] is used as an effective nucleon-nucleon interaction (v_{NN}), and proton-neutron mass difference is ignored. In other words, we only consider the Coulomb interaction as the source of isospin symmetry breaking. This simplification may be validated in the case of ^{14}N which we will discuss later, because the Coulomb interaction should dominate over other symmetry breaking terms.

The variational wave function is a parity-projected Slater determinant,

$$\Phi^\pi = \hat{P}^\pi \mathcal{A}\{\varphi_1 \varphi_2 \dots \varphi_A\}, \quad \pi = \pm \quad (2)$$

where \hat{P}^π is the parity projection operator. The single-particle wave packet φ_i is represented by a deformed Gaussian [15],

$$\varphi_i(\mathbf{r}) = \prod_{\sigma=x,y,z} e^{-\nu_\sigma(r_\sigma - Z_{i\sigma})^2} \chi_i \eta_i, \quad (3)$$

$$\chi_i = a_i \chi_\uparrow + b_i \chi_\downarrow, \quad \eta_i = \{ \text{proton or neutron} \}. \quad (4)$$

The variational parameters are the width (ν_x, ν_y, ν_z) and the centroids \mathbf{Z}_i of Gaussian wave packets, and spin direction a_i and b_i . They are determined by the energy variation with the

constraint on the matter quadrupole deformation parameter β . We denote the wave function obtained by the energy variation as $\Phi^\pi(\beta)$ which has the minimum energy for given value of the parameter β . Note that the energy variation tends to yield the wave functions with minimum isospin as they are energetically favored. In short, the energy variation produces wave functions with $T = 0$ for ^{14}N and those with $T = 1$ for ^{14}C .

B. Basis wave functions for isobaric analog states

As explained above, it is not straightforward to obtain the wave functions of isobaric analog states, e.g., the $T = 1$ states of ^{14}N , by the energy variation. Here, we propose a simple method to generate the basis wave functions for describing the isobaric analog states. Let us explain it by using the $T = 1$ states of ^{14}N as examples. Suppose that we have obtained the wave function of ^{14}C by the energy variation,

$$\Phi^\pi(\beta, ^{14}\text{C}(T = 1)) = P^\pi \mathcal{A} \{ \varphi_1 \cdots \varphi_6 \varphi_7 \cdots \varphi_{14} \}, \quad (5)$$

where $\varphi_1 \cdots \varphi_6$ and $\varphi_7 \cdots \varphi_{14}$ are the proton and neutron single-particle wave packets, respectively. Note that this wave function is mostly composed of the $T = 1$ component (minimum isospin for ^{14}C). Then, we simply apply the Fermi transition operator of β^- decay to produce the wave function of ^{14}N ,

$$\begin{aligned} \Phi^\pi(\beta, ^{14}\text{N}(T = 1)) &= T^+ \Phi^\pi(\beta, ^{14}\text{C}(T = 1)) \\ &= \sum_{i=7}^{14} P^\pi \mathcal{A} \{ \varphi_1 \cdots \varphi_6 \varphi_7 \cdots \varphi_i \cdots \varphi_{14} \}, \end{aligned} \quad (6)$$

where i th neutron wave packet ($i = 7, \dots, 14$) is turned into proton. Since T^+ commutes with T^2 , this wave function approximates isobaric analog state ($T = 1$ states) of ^{14}N . We propose to use each term of Eq. (6) as the basis wave function for generator coordinate method. Thus, we generate eight wave functions for ^{14}N from a single ^{14}C wave function, which are denoted as,

$$\begin{aligned} \Phi_i^\pi(\beta, ^{14}\text{N}(T = 1)) &= t_i^+ \Phi^\pi(\beta, ^{14}\text{C}(T = 1)) \\ &= P^\pi \mathcal{A} \{ \varphi_1 \cdots \varphi_6 \varphi_7 \cdots \varphi_i \cdots \varphi_{14} \}. \end{aligned} \quad (7)$$

C. Generator coordinate method

Once the basis wave functions are prepared, we perform the angular momentum projection and GCM calculation. The basis wave functions are projected to the eigenstates of the angular momentum and superposed,

$$\begin{aligned}\Psi_M^{J\pi} = & \sum_{\beta K} f_{\beta K} P_{MK}^J \Phi^\pi(\beta, {}^{14}\text{N}(T=0)) \\ & + \sum_{\beta Ki} g_{\beta Ki} P_{MK}^J \Phi_i^\pi(\beta, {}^{14}\text{N}(T=1)),\end{aligned}\quad (8)$$

where P_{MK}^J is angular momentum projection operator. Note that $\Phi^\pi(\beta, {}^{14}\text{N}(T=0))$ are obtained by the energy variation and mainly consist of $T=0$ components whereas $\Phi_i^\pi(\beta, {}^{14}\text{N}(T=1))$ are generated by Eq. (7) and predominated by $T=1$ components. The eigen-energies and the coefficients of superposition $f_{\beta K}$ and $g_{\beta Ki}$ are determined by solving the Hill-Wheeler equation [16].

III. RESULTS AND DISCUSSION

Figure 1 shows the energy curves of ${}^{14}\text{N}$ and ${}^{14}\text{C}$ as functions of the quadrupole deformation parameter β which are obtained by the energy variation after the parity projection. The positive-parity states have the spherical energy minimum with $N=8$ closed shell for

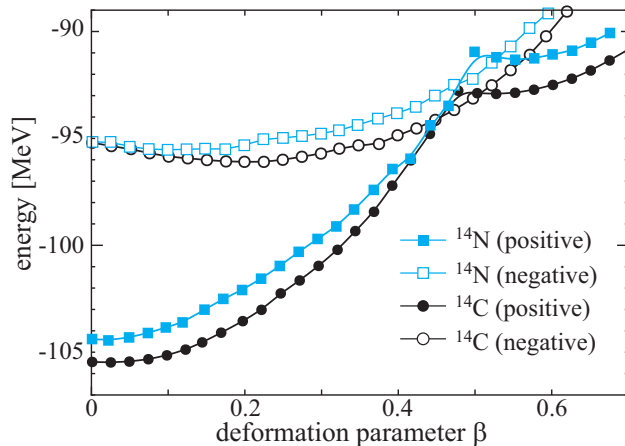


FIG. 1. Energy curves for ${}^{14}\text{N}$ and ${}^{14}\text{C}$ as functions of the quadrupole deformation parameter β obtained by the energy variation after parity projection.

${}^{14}\text{C}$ and a single neutron hole for ${}^{14}\text{N}$ which are the dominant components of the ground

states. As quadrupole deformation grows, the energy increases rapidly and the level crossing occurs creating energy plateau around $\beta = 0.6$. In this plateau, both nuclei have two-particle and two-hole ($2p2h$) configurations which generate the highly excited states [17, 18]. The negative-parity energy curves are located at much higher energy than the positive-parity states as they involve particle-hole excitation across the $N = Z = 8$ shell gap. Although it is not clear from the shape of the energy curves, the negative-parity states have $1p1h$ configurations in the small deformation region, and $3p3h$ configurations in the largely deformed region. Thus, both nuclei have similar behavior of the energy curve due to the similarity in the single particle configurations. The energy difference between ^{14}N and ^{14}C is due to the difference in the isospin channel ($T = 0$ for ^{14}N and $T = 1$ for ^{14}C) and the Coulomb interaction.

As explained in the previous section, we apply the Fermi transition operator of β^- decay to the wave functions of ^{14}C (circles in Fig. 1) to yield the wave functions of ^{14}N with $T = 1$. The wave functions thus-generated are superposed with the wave functions of ^{14}N with $T = 0$ (squares in Fig. 1) to perform the GCM calculations.

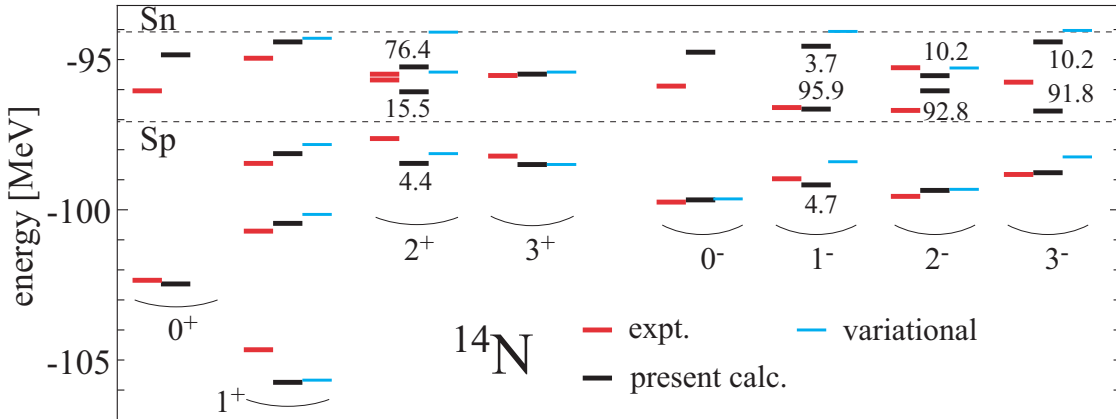


FIG. 2. Calculated and observed level scheme of ^{14}N up to $J^\pi \leq 3^\pm$. Black lines show the result of the present model whereas blue lines show the results calculated by using only the variationally obtained basis wave functions. Numbers in the figure shows the amount of the $T = 1$ component in percentage for the states with sizable isospin mixing.

The spectra of ^{14}N obtained by the GCM calculations are shown in Figure 2. By using only the variationally obtained wave functions of ^{14}N (without the $T = 1$ wave functions generated from ^{14}C), the GCM calculation (blue lines in Fig. 2) fails to reproduce several

excited states such as the $0_{1,2}^+, 0_2^-$ and 1_2^- states, all of which are $T = 1$ states. Thus, the variational calculations energetically favor the $T = 0$ states and leaves out the $T = 1$ states. On the contrary, by adding the basis wave functions generated by applying the Fermi transition operator to the ^{14}C wave functions, the present model plausibly describes both $T = 0$ and 1 states (black lines). Note that the all the observed states up to $E_x < 10$ MeV are reasonably reproduced by our simple method, although the calculation slightly overestimate the binding energy of the ground state. To elucidate the accuracy of the present calculations, Table I shows the electromagnetic properties of the $1_{1,2}^+$ ($T = 0$) and 0_1^+ ($T = 1$) states. It is encouraging that the present calculation reproduces not only the electromagnetic moments of the individual states but also the transition probabilities between $T = 0$ and 1 states [19]. Thus, our proposed method is simple but accurately describes both of the $T = 0$ and 1 states with a small computational cost.

TABLE I. The calculated and observed [19] properties of the low-lying 1^+ and 0^+ states. Excitation energy, magnetic dipole and electric quadrupole moments are given in the unit of MeV, μ_N and efm^2 , respectively. The $M1$ and $E2$ reduced transition probabilities are given in the Weisskopf unit.

J^π	E_x		μ		Q	
	calc.	exp.	calc.	exp.	calc.	exp.
$1_1^+(T = 0)$	0.0	0.0	0.39	0.40	1.7	1.9
$1_2^+(T = 0)$	3.2	2.3	0.45	0.39	0.8	—
$0_1^+(T = 1)$	4.9	3.9	—	—	—	—
$B(M1)$			$B(E2)$			
$J_i^\pi \rightarrow J_f^\pi$	calc.	exp.	calc.	exp.	calc.	exp.
$1_1^+ \rightarrow 0_1^+$	0.023	0.026	—	—	—	—
$1_2^+ \rightarrow 0_1^+$	1.2	1.0	—	—	—	—
$1_1^+ \rightarrow 0_2^+$	3.3×10^{-4}	1.4×10^{-4}	2.2	2.7	—	—

Now, we discuss the isospin mixing described by our model. The present calculation yielded several states with sizable isospin mixing, for which we showed the mixing ratio (amount of the $T = 1$ component in percentage) in Fig. 2. It is notable that the states close

to the $^{13}\text{C} + p$ or $^{13}\text{N} + n$ threshold energies have strong isospin mixing, which is related to the origin of the isospin mixing as explained below.

TABLE II. The electric and magnetic dipole transition strengths for the 1_1^- and 1_2^- states [4, 19] given in Weisskopf unit.

$J_i^\pi \rightarrow J_f^\pi$	$ \Delta T $	$B(E1)_{\text{exp}}$	$B(E1)_{\text{calc}}$
$1_1^- \rightarrow 0_1^+$	1	$\geq 2.4 \times 10^{-3}$	3.2×10^{-3}
$1_1^- \rightarrow 1_1^+$	0	$\geq 2.3 \times 10^{-4}$	1.8×10^{-4}
$1_1^- \rightarrow 1_2^+$	0	-	1.5×10^{-4}
$1_2^- \rightarrow 0_1^+$	0	$(2.3 \pm 0.7) \times 10^{-3}$	1.6×10^{-3}
$1_2^- \rightarrow 1_1^+$	1	$(4.8 \pm 1.2) \times 10^{-2}$	3.6×10^{-2}
$1_2^- \rightarrow 1_2^+$	1	$(5.7 \pm 1.5) \times 10^{-2}$	3.4×10^{-2}
$J_i^\pi \rightarrow J_f^\pi$	$ \Delta T $	$B(M1)_{\text{exp}}$	$B(M1)_{\text{calc}}$
$1_1^- \rightarrow 0_1^-$	0	-	0.01
$1_1^- \rightarrow 2_1^-$	0	-	0.06
$1_2^- \rightarrow 0_1^-$	1	1.6	1.6
$1_2^- \rightarrow 1_1^-$	1	0.06	0.17
$1_2^- \rightarrow 2_1^-$	1	0.36	0.36

Among these states, the 1_1^- (5.69 MeV, $T = 0$) and 1_2^- (8.06 MeV, $T = 1$) states are well-known example of the isospin mixing for which the mixing ratio was evaluated experimentally [4]. In the following, we discuss how these states are described by our model and anatomy their structure. Table II lists the electric and magnetic dipole transition probabilities of these 1^- states. Firstly, note that the experimental values of the electric and magnetic dipole transition strengths of the 1^- states are reproduced accurately. This indicates that our model precisely describes the wave functions of the 1^- states. Secondly, we should focus on the intensities of the $E1$ transition strengths. Since ^{14}N is a self-conjugate nucleus, isospin selection rule allows only $|\Delta T| = 1$ transitions and forbids the $|\Delta T| = 0$ transitions [1]. In fact, the $|\Delta T| = 0$ transitions are suppressed by an order of magnitude compared to the $|\Delta T| = 1$ transitions for both observed and calculated values. At the same time, non-zero values for the $|\Delta T| = 0$ transitions indicate the isospin mixing in the 1_1^- and 1_2^- states. In Ref. [4], the mixing ratio was estimated from the $E1$ transition probabilities.

They assumed that the $1_{1,2}^+$ and 0_1^+ have no isospin mixing and the $1_{1,2}^-$ states are admixture of two components as,

$$\Psi(1_1^-) = \alpha\Phi(1) + \beta\Phi(0), \quad (9)$$

$$\Psi(1_2^-) = \beta\Phi(1) - \alpha\Phi(0), \quad (10)$$

where $\Phi(0)$ and $\Phi(1)$ denote the $T = 0$ and 1 wave functions. Then, the ratio of the allowed and forbidden transitions gives an estimate of the mixing ratio as,

$$\frac{B(E1)_{\text{forbidden}}}{B(E1)_{\text{allowed}}} = \frac{\alpha^2}{\beta^2} = \frac{\alpha^2}{1 - \alpha^2}. \quad (11)$$

They adopted the observed $1_2^- \rightarrow 1_1^+$ and $1_2^- \rightarrow 0_1^+$ transition strengths and obtained an estimate of $\alpha_{\text{exp}}^2 = 0.046$ whereas our calculated transition strengths yield $\alpha_{\text{calc}}^2 = 0.042$, both of which are close to the mixing ratio directly calculated from our 1^- wave functions ($\alpha^2 = 0.047$ for 1_1^- and 0.041 for 1_2^-). Other combinations of the transition strengths also suggest similar values, for example, $1_1^- \rightarrow 1_1^+$ and $1_1^- \rightarrow 0_1^+$ transitions give $\alpha_{\text{exp}}^2 = 0.09$ and $\alpha_{\text{calc}}^2 = 0.053$.

In order to understand the origin of isospin mixing, we investigate the spectroscopic factors and the overlap functions. We calculate the overlap between the wave function of ^{14}N with the spin-parity $J^{\pi'}$ and that of ^{13}N with J^π [20],

$$\varphi(\mathbf{r}) = \sqrt{13} \langle \Psi_{M'-m}^{J^\pi}(^{13}\text{N}) | \Psi_{M'}^{J^{\pi'}}(^{14}\text{N}) \rangle. \quad (12)$$

The overlap function is given as the multipole decomposition of $\varphi(\mathbf{r})$,

$$\varphi_{jl}(r) = \int d\hat{r} [Y_l(\hat{r}) \times \chi_{1/2}]_{jm}^\dagger \varphi(\mathbf{r}), \quad (13)$$

which is the radial wave function of a valence neutron in the $J^\pi \otimes \nu(l_j)$ channel. The spectroscopic factor is the norm of $\varphi_{jl}(r)$,

$$S(J^\pi \otimes \nu(l_j)) = \int r^2 dr |\varphi_{jl}(r)|^2. \quad (14)$$

The spectroscopic factors in the $J^\pi \otimes \pi(l_j)$ channels (the overlap between ^{14}N and ^{13}C) are also calculated in the same manner. The calculated spectroscopic factors and the overlap functions of the 1^- states are given in Table III and Fig. 3, respectively. For comparison, we also present spectroscopic factors for the $1_1^+(T = 0)$ and $0_1^+(T = 1)$ states which have no isospin mixing. If we assume that both ^{13}C and ^{13}N are the eigenstates of isospin with

TABLE III. The spectroscopic factors of the 1_1^+ , 0_1^+ and $1_{1,2}^-$ states in the $J^\pi \otimes \nu(l_j)$ and $J^\pi \otimes \pi(l_j)$ channels, where J^π denotes the spin-parity of ^{14}N and ^{14}C whereas l_j denotes the orbital and total angular momenta of a valence neutron or proton.

	$\frac{1}{2}^- \otimes \nu(p_{1/2})$	$\frac{1}{2}^- \otimes \pi(p_{1/2})$	$\frac{5}{2}^- \otimes \nu(p_{3/2})$	$\frac{5}{2}^- \otimes \pi(p_{3/2})$
1_1^+	0.87	0.87	1.28	1.29
	$\frac{1}{2}^- \otimes \nu(p_{1/2})$	$\frac{1}{2}^- \otimes \pi(p_{1/2})$	$\frac{3}{2}^- \otimes \nu(p_{3/2})$	$\frac{3}{2}^- \otimes \pi(p_{3/2})$
0_1^+	0.90	0.90	0.99	1.04
	$\frac{1}{2}^- \otimes \nu(s_{1/2})$	$\frac{1}{2}^- \otimes \pi(s_{1/2})$	$\frac{1}{2}^+ \otimes \nu(p_{1/2})$	$\frac{1}{2}^+ \otimes \pi(p_{1/2})$
1_1^-	0.23	0.43	0.47	0.25
1_2^-	0.38	0.23	0.28	0.42

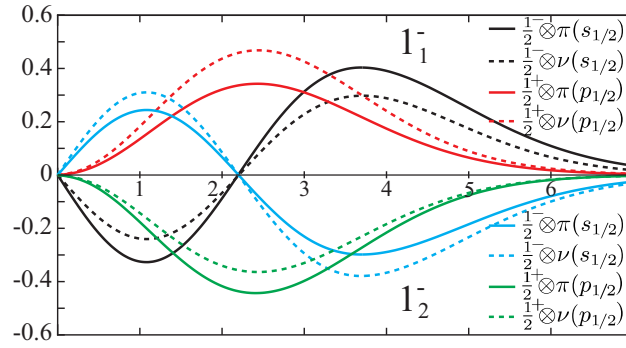


FIG. 3. The overlap functions of the 1_1^+ , 0_1^+ and $1_{1,2}^-$ states in the $J^\pi \otimes \nu(l_j)$ and $J^\pi \otimes \pi(l_j)$ channels. The phases of the overlap functions are arbitrary chosen for the presentation.

$T = 1/2$, which is a reasonable assumption indeed, the spectroscopic factors in the $J^\pi \otimes \nu(l_j)$ and $J^\pi \otimes \pi(l_j)$ channels should be equal for the pure $T = 0$ or 1 states. In fact, we see the equality holds for the low-lying 1_1^+ and 0_1^+ states. However, we found that the spectroscopic factors for the 1_1^- and 1_2^- states show significant asymmetry between two channels because of the isospin mixing. The 1_1^- state has larger contribution from the $1/2^- \otimes \pi(s_{1/2})$ and the $1/2^+ \otimes \nu(p_{1/2})$ channels compared to the $1/2^- \otimes \nu(s_{1/2})$ and the $1/2^+ \otimes \pi(p_{1/2})$ channels, whereas the 1_2^- state shows the opposite trend.

The origin of the asymmetry is understood as follows. Notice that $^{13}\text{N}(1/2^-)$ and $^{13}\text{N}(1/2^+)$ are approximated as the $\nu(p_{1/2})$ and $\nu(s_{1/2})$ states on top of the ^{12}C ground state as an inert core. The same also applies to $^{13}\text{C}(1/2^\pm)$. So, we see that both $1/2^- \otimes \nu(s_{1/2})$ and

$1/2^+ \otimes \pi(s_{1/2})$ channels are identically represented as $\pi(s_{1/2})\nu(p_{1/2})$. In the same manner, $1/2^+ \otimes \nu(s_{1/2})$ and $1/2^- \otimes \pi(p_{1/2})$ are represented as $\pi(p_{1/2})\nu(s_{1/2})$. Hence, we understand that Tab. III implies that the 1_1^- and 1_2^- are approximated by the linear combinations of $1p1h$ excitation across the $N = Z = 8$ shell gap,

$$|1_1^- \rangle = a |\pi(s_{1/2})\nu(p_{1/2}) \rangle - b |\pi(p_{1/2})\nu(s_{1/2}) \rangle, \quad (15)$$

$$|1_2^- \rangle = b |\pi(s_{1/2})\nu(p_{1/2}) \rangle + a |\pi(p_{1/2})\nu(s_{1/2}) \rangle, \quad (16)$$

with $a > b$, which is consistent with the assumption made in the shell model calculations [21–24]. Since the ground state of ^{14}N be approximated as $\pi(p_{1/2})\nu(p_{1/2})$, this indicates that the proton excitation $\pi(p_{1/2} \rightarrow s_{1/2})$ is energetically favored over the neutron excitation $\nu(p_{1/2} \rightarrow s_{1/2})$. This owes to the Coulomb energy difference. As shown in Fig. 3, the $\pi(s_{1/2})$ orbit is spatially extended than $\pi(p_{1/2})$ as it is close to the threshold energy. Consequently, $\pi(s_{1/2})$ has smaller Coulomb repulsion than $\pi(p_{1/2})$, and hence, the single-particle excitation energy which costs for $\pi(p_{1/2} \rightarrow s_{1/2})$ is reduced than that for $\nu(p_{1/2} \rightarrow s_{1/2})$. We also found that other excited states with isospin mixing such as $2_{1,2,3}^+$, $2_{2,3}^-$ and $3_{2,3}^-$ states always involve the single-particle excitation to $s_{1/2}$. Therefore, we conclude the Coulomb energy shift of proton $s_{1/2}$ orbit is a major source of the isospin mixing in the excited states close to the proton and neutron decay thresholds.

IV. SUMMARY

In this work, we proposed a tractable method to describe the isospin mixing within a framework of generator coordinate method. By applying the Fermi transition operator to the wave functions of isobars, we generated the wave functions of the isobaric analog states which are used as the basis of GCM calculations. Using ^{14}N as an example, we demonstrated that our tractable method plausibly describes both of $T = 0$ and 1 states and the isospin mixing in the excited states close to the proton and neutron thresholds. We showed that our model reasonably describes the strengths of the allowed and forbidden $E1$ transitions that are consistent with the mixing ratio. Furthermore, based on the spectroscopic factors and overlap functions, we deduced that the Coulomb energy shift of $s_{1/2}$ orbit is a major source of the isospin mixing.

ACKNOWLEDGMENTS

This work was supported by the JSPS KAKENHI Grant No. 19K03859. Part of the numerical computation in this work was carried out at the Yukawa Institute Computer Facility.

- [1] E. K. Warburton and J. Weneser, *Isospin in Nuclear Physics*, edited by D. H. Wilkinson (North-Holland, Amsterdam, 1969).
- [2] A. Bohr and B. Mottelson, *Nuclear Structure Vol. 1* (Benjamin Inc., New York, 1969).
- [3] F. C. Barker, *Nuclear Physics* **83**, 418 (1966).
- [4] M. J. Renan, J. P. Sellschop, R. J. Keddy, and D. W. Mingay, *Nuclear Physics A* **193**, 470 (1972).
- [5] C. Rolfs and W. Rodney, *Cauldrons in the Cosmos: Nuclear Astrophysics, Rolfs, Rodney* (University of Chicago Press, Chicago, 1988).
- [6] S. E. Woosley, A. Heger, and T. A. Weaver, *Rev. Mod. Phys.* **74**, 1015 (2002).
- [7] R. J. Deboer, J. Görres, M. Wiescher, R. E. Azuma, A. Best, C. R. Brune, C. E. Fields, S. Jones, M. Pignatari, D. Sayre, K. Smith, F. X. Timmes, and E. Uberseder, *Reviews of Modern Physics* **89** (2017), 10.1103/REVMODPHYS.89.035007/FIGURES/2/THUMBNAIL.
- [8] W. Satuła and R. Wyss, *Physical Review Letters* **86**, 4488 (2001).
- [9] K. Sato, J. Dobaczewski, T. Nakatsukasa, and W. Satuła, *Physical Review C* **88**, 061301 (2013).
- [10] Y. Kanada-En'yo, H. Morita, and F. Kobayashi, *Physical Review C* **91**, 054323 (2015).
- [11] P. Bączyk, J. Dobaczewski, M. Konieczka, W. Satuła, T. Nakatsukasa, and K. Sato, *Physics Letters B* **778**, 178 (2018).
- [12] W. Satuła, J. Dobaczewski, W. Nazarewicz, and M. Rafalski, *Physical Review C - Nuclear Physics* **81** (2010), 10.1103/PHYSREVC.81.054310.
- [13] H. Morita and Y. Kanada-En'yo, *Progress of Theoretical and Experimental Physics* **2016**, 103 (2016).
- [14] J. F. Berger, M. Girod, and D. Gogny, *Computer Physics Communications* **63**, 365 (1991).
- [15] M. Kimura, *Physical Review C* **69**, 044319 (2004).
- [16] D. L. Hill and J. A. Wheeler, *Physical Review* **89**, 1102 (1953).

- [17] T. Suhara and Y. Kanada-En'yo, Physical Review C **82**, 044301 (2010).
- [18] T. Baba and M. Kimura, Physical Review C **94**, 044303 (2016).
- [19] F. Ajzenberg-Selove, Nuclear Physics A **523**, 1 (1991).
- [20] M. Kimura, Physical Review C **95** (2017), 10.1103/PhysRevC.95.034331.
- [21] E. K. Warburton and W. T. Pinkston, Physical Review **118**, 733 (1960).
- [22] T. Sebe, Progress of Theoretical Physics **30**, 290 (1963).
- [23] S. T. Hsieh and H. Horie, Nuclear Physics A **151**, 243 (1970).
- [24] H. U. Jäger, H. R. Kissener, and R. A. Eramzhian, Nuclear Physics A **171**, 16 (1971).